Robust point-to-point trajectory planning for nonlinear underactuated systems: theory and experimental assessment

Paolo Boscariol[1], Dario Richiedei

Dipartimento di Tecnica e Gestione dei sistemi Industriali - DTG
Università degli Studi di Padova, Stradella S. Nicola 6, 36100 Vicenza, Italy

Abstract

This paper proposes the theory and the experimental assessment of a robust model-based trajectory planning algorithm for underactuated nonlinear systems in point-to-point motion. The method has been developed to increase the insensitivity of the resulting trajectory to parametric uncertainties of the plant. The proposed method is based on an augmented model that considers an approximate dynamics of the servo-controlled axis driving the actuated degrees of freedom. Trajectory planning is accomplished by computing the motion reference for the actuated degrees of freedom to reduce the effects of the uncertainty on the dynamic model. By exploiting an indirect variational formulation method, the necessary optimality conditions deriving from the Pontryagin's minimum principle are imposed, thus leading to a differential Two-Point Boundary Value Problem (TPBVP). Numerical solution of the latter is accomplished by means of collocation techniques to handle model nonlinearities.

Robustness is achieved by including additional conditions on the sensitivity functions for the initial and final points of the trajectory. The experimental evaluation of the effectiveness of the proposed method is performed on a double-pendulum crane, by comparing the transient and residual vibration. A comparison is provided with three well-established input-shaping methods, and robustness against unmodeled parametric perturbations and tracking errors is evaluated. The experimental evidence indicates that the inclusion of the additional constrains results in an effective reduction of the residual vibration, and that the proposed method is well suited to perform high speed motion.

Keywords:
model-based trajectory planning, smooth trajectory, trajectory planning, underactuated system

1. Introduction

High-speed operation of robotic manipulators and automatic machines requires the concurrent use of effective control systems and smooth trajectories to ensure accurate tracking of the desired reference with minimum vibration excitation. The problem of motion-induced vibration is exacerbated in underactuated systems, such as cranes or machines with a lightweight construction of either the links or the joints [1, 2]. Such manipulators might incur in severe vibration both during the motion and after motion completion, thus limiting their operativeness and their precision [3].

The literature proposes several approaches to improve the dynamic behavior of underactuated systems. Focusing on trajectory planning can reduce the need for accurate, high-bandwidth sensors devoted to vibration control. This feature is useful in those industrial applications where the use of additional sensor can be impractical or non cost-effective, as well as those where the system is controlled by standard, closed and proprietary industrial controllers. This fact has been attracting a lot of attention in the scientific community and among industrial practitioners.

Email address: `paolo.boscariol@unipd.it` (Paolo Boscariol)

The literature on trajectory planning algorithms is therefore quite extensive, as shown by the review paper [4]. A first distinction can be made between model-free and model-based approaches. The first approach is a general strategy that has the advantage of allows the same technique to be applied to several different machines without any knowledge of their dynamic model.

Model-free trajectory planning algorithms are often based on geometric approaches, and therefore they focus on the definition of time laws defined either in the joint space or in the operational space [5] using interpolation techniques. Vibration reduction is achieved by reducing or eliminating jerk peaks, which are responsible for the excitation of the mechanical structure of the machine [6]. Acceleration continuity and jerk limitation is obtained by choosing suitable motion primitives, such as B-splines [7, 8] or cubic splines [9]. Their effectiveness is however limited to the possibility of reducing vibration excitation, since in general they cannot guarantee zero residual vibration.

In contrast, model-based approaches requires an adequate knowledge of the dynamics of the model for which the trajectory is planned. Therefore, they can generally lead to more accurate results and zero residual vibrations, at the cost of a lesser robustness to model-plant mismatches, unless uncertainty is properly tackled in the design. A model can be used in the design by following several approaches. For example, zero residual vibration can be achieved by precise timing of motion laws such as s-curve speed profiles [10] or smoothed jerk profiles [11], by taking advantage of the knowledge of frequencies and damping factors of the main vibrational modes.

The same concept is exploited also for the class of methods referred to as input shaping, which have gained a wide diffusion [12, 13] due to their effectiveness and simple implementation and are often used as benchmarks in the literature. Input shaping filters can be used to perform rest-to-rest motion with zero residual vibration for single mode [14] and multi-mode systems [15].

Input shaping techniques have also been extended to react to uncertainty or changes of the oscillation frequencies, leading to the definition of robust shapers and to the extra-insensitive robust shapers [16].

Similar performances levels can be achieved by translating the motion profile design into a filter design problem, that are used to produce smooth motion profiles when convolved with rough reference signals (see e.g. [17, 18]).

An alternative approach to model-based trajectory planning is based on translating it as the solution of an optimal control problem. Among the extensive literature on such a topic, a main distinction can be made into direct and indirect optimization methods.

In the case of direct methods, the original optimal control problem is converted into a parameter optimization problem [19], by a proper discretization of robot kinematic variables. Then this new finite-dimensional problem can be solved through a wide number of efficient optimization algorithm, either deterministic or stochastic ones. For example, an optimization problem is solved in [20] to compute the coefficients which define the correct zero residual vibration as a combination of polynomial and cycloidal functions. In such a work, as wells as in others using direct methods such as [21], the solution of the optimization problem imposes extensive dynamic simulations and therefore they require a non-negligible computational effort. Hence, their effectiveness is reduced in the presence of systems with large number of degrees of freedom [22].

Indirect methods make use of calculus of variations: the necessary conditions of the Pontryagin's Minimum Principle (PMP) are imposed and the resulting Two-Point Boundary Value Problem (TP-BVP) is solved. Indirect methods are widely reckoned to be very accurate, particularly in the case of high degree of underactuation or multi-objective optimization [23]. Their application is very widespread in literature, and they have used for mobile robot application [24], flexible-joints robots [25], flexible-link robots [26] and cable-based robots [27], just to cite a few examples.

The general framework of calculus of variations can be adapted to include countless options in the optimization problem, and to account for constraints as well, which are always useful when addressing practical implementations.

One of the main drawbacks of this approach, that is inherited from its roots in optimal control, is the limited robustness to parametric mismatches between the plant used for the planning and the actual plant. Robustness to such changes is, instead, a highly useful characteristic that should be achieved by any control scheme or trajectory planning algorithm [28]. Therefore, the robustness

issued has been tackled extensively in the field of closed-loop control, as testified by a literature too vast to be referenced in this work, but to the best of authors knowledge, there are very few works that specifically focus on robust trajectory planning algorithms.

One example is [29], in which robustness is achieved by introducing in the cost function a term of Gaussian cumulative noise. The work by Shin [30] focuses on the definition of robot trajectories by taking into account the uncertainties brought by payload variations trough the change of bounds on joint torques. Other interesting approaches to robust trajectory planning are currently available as solutions to the problem of robust optimization for dynamic systems: an extensive overview of this problem is available in [31]. One of the Authors of the present paper has recently proposed an extension of the variational approach to trajectory planning problems that can cope with parametric uncertainties [32], that unlike other methods in literature (such as those in [33, 34]), can cope with plants described by nonlinear dynamics.

Model-based techniques casting optimal motion planning as an optimal control problem can be also grouped in accordance with the variables obtained as the output. For example, papers [35, 36, 37] compute the optimal profile of the command force (or torque) driving the actuated degrees of freedom, by casting, in practice, optimal motion planning as an inverse dynamics problem. A less common approach is, instead, performing optimal trajectory planning by synthesizing the optimal position (or speed) reference of the actuated degrees of freedom, such as the one in [38, 39, 40]. Although such an approach has attracted less attention, it has some practical advantages that make it suitable for the implementation in industrial robots or manipulators, as well as in complicate multibody systems. Indeed, it does not require estimating the control force needed to perform the motion, which are instead computed by the real-time feedback and feedforward control of the axis driving the underactuated system.

Experimental validation of the method is also provided through a double pendulum crane system, which is a three degree of freedom system described by a set of nonlinear differential equations. The experimental testbed is developed through an industrial robot with proprietary and closed controller, thus corroborating the ease of implementation in real systems. A comparison with three widely used input shaping techniques is provided as well.

2. System model formulation

The equations of motion of a multibody system with n degrees of freedom (dofs) can be written, given a proper choice of of n independent coordinates $\mathbf{q}$, as the set of n nonlinear ordinary differential equations:

$$\mathbf{M}(\mathbf{q}) = \mathbf{K}(\mathbf{q}) + \mathbf{G}(\mathbf{q}, \dot{\mathbf{q}}) + \mathbf{B}(\mathbf{q})\mathbf{F} \tag{1}$$

$\mathbf{M} \in \Re^{m \times n}$ is the mass matrix, $\mathbf{K} \in \Re^{n}$ is the vector of position-dependent forces, i.e. elastic and gravity forces. Vector $\mathbf{G} \in \Re^{n}$ takes into account the gyroscopic and the centrifugal forces, as well as the damping forces. $\mathbf{B} \in \Re^{n \times m}$ is the force distribution vector, which weights the effect of the external control forces $\mathbf{F} \in \Re^{m}$. If $m < n$ the system is said to be underactuated, i.e. the number of the control forces is less than the size of the vector of the generalized coordinates. Hence $\mathbf{B}$ cannot be inverted. The dynamic model in Eq. (1) can be conveniently partitioned to highlight the contributions related to the m actuated coordinates $\mathbf{q}_a$ and the $n - m$ unactuated ones $\mathbf{q}_u$:

$$\begin{bmatrix} \mathbf{M}_{aa} & \mathbf{M}_{au} \\ \mathbf{M}_{au}^T & \mathbf{M}_{uu} \end{bmatrix} \begin{bmatrix} \ddot{\mathbf{q}}_a \\ \ddot{\mathbf{q}}_u \end{bmatrix} = \begin{bmatrix} \mathbf{K}_a(\mathbf{q}) \\ \mathbf{K}_u(\mathbf{q}) \end{bmatrix} + \begin{bmatrix} \mathbf{G}_a(\mathbf{q}, \dot{\mathbf{q}}) \\ \mathbf{G}_u(\mathbf{q}, \dot{\mathbf{q}}) \end{bmatrix} + \begin{bmatrix} \mathbf{B}_a \\ 0 \end{bmatrix} \mathbf{F} \tag{2}$$

This partition shows that the motion of the unactuated coordinates is determined by the motion of the actuated ones as:

$$\ddot{\mathbf{q}}_u = \mathbf{M}_{uu}^{-1} \left(\mathbf{K}_u + \mathbf{G}_u \right) - \mathbf{M}_{uu}^{-1} \mathbf{M}_{au}^T \ddot{\mathbf{q}}_a \tag{3}$$

Conversely, the actuated coordinates can be forced to follow a prescribed trajectory $\mathbf{q}_a^{ref}$ by choosing a proper control force profile, which is usually determined by the control scheme adopted.

The availability of high-bandwidth closed loop control schemes, together with feedforward actions, can boost correct tracking of the desired trajectory for the actuated dofs. Under these circumstances, as often done in literature (see e.g. [41, 42, 2], just to mention a few notable examples), perfect tracking can be assumed, i.e. the actual trajectory is assumed to be equal to the planned one: $\mathbf{q}_a(t) = \mathbf{q}_a^{ref}(t)$.

An improved approach is instead proposed in this paper by assuming a dynamic relationship between the desired and the actual trajectories of the actuated dofs, that might be expressed through function $\mathbf{h}$:

$$\ddot{\mathbf{q}}_a(t) = \mathbf{h}(\ddot{\mathbf{q}}_a^{ref}(t)) \tag{4}$$

Function $\mathbf{h}$ is, in general, an approximation of the actual closed-loop dynamics of the system, that represents the dynamic behavior of both the actuators and the controller. Under this hypothesis, the system can be described as a first order system of ODEs, with $\ddot{\mathbf{q}}_a^{ref}$ as the exogenous input, and with $\mathbf{q} = [\dot{\mathbf{q}}_u^T, \dot{\mathbf{q}}_a^T]^T$ as the state vector:

$$\begin{bmatrix} \ddot{\mathbf{q}}_u \\ \ddot{\mathbf{q}}_a \end{bmatrix} = \begin{bmatrix} \mathbf{M}_{uu}^{-1}\left(\mathbf{K}_u(\mathbf{q}) + \mathbf{G}_u(\mathbf{q}, \dot{\mathbf{q}})\right) \\ 0 \end{bmatrix} + \begin{bmatrix} -\mathbf{M}_{uu}^{-1}\mathbf{M}_{au}^T \\ \mathbf{I} \end{bmatrix} \mathbf{h}(\ddot{\mathbf{q}}_a) \tag{5}$$

This model is different from the one proposed in [32] where motion planning is cast as an inverse dynamic problem based on the dynamic model of the whole system of Eq. (1). The use of such a dynamic model with the control forces of the actuated dofs as the control input leads to the computation of the optimal forces. Hence, it is suitable for control schemes operating in current control configuration, which are however of less common used. In contrast, the model formulation adopted in this work casts motion planning as the synthesis of the optimal reference for the actuated dofs, namely $\mathbf{q}_a^{ref}$ and its time derivatives. This different approach is justified by practical considerations. First, industrial controllers are often developed as "closed" and proprietary systems that cannot be modified. In these cases, vibration control can be accomplished by just setting the suitable motion reference for the actuated dofs (together with a wise tuning of the controller gains). Then, the forces required to perform the prescribed motion are computed by the axis controllers of the actuated dofs, through the feedback and the feedforward contributions. This second important feature gets rid of unmodeled dynamics, such as frictions and unknown external forces, which might introduce severe steady-state errors in the final positioning in the case of computed force approaches. Hence, robustness issues are less severe and additional robustness properties of the trajectories developed should be be ensured with respect to a few critical parameters.

A practical approach for implementing Eq. (5) is to approximate the dynamics of the controlled DOFs, i.e. function $\mathbf{h}$, through a few dominant poles of the controlled system. An effective approach is for example assuming a first-order linear and time-invariant model, with unitary gain and a positive time constant τ representing the zero steady-state error and the limited bandwidth:

$$\dddot{\mathbf{q}}_a(t) = -\frac{1}{\tau}\ddot{\mathbf{q}}_a(t) + \frac{1}{\tau}\ddot{\mathbf{q}}_a^{ref}(t) \tag{6}$$

The inclusion of Eq. (6) into Eq. (5) requires augmenting the state vector with $\ddot{\mathbf{q}}_a$ as follows:

$$\begin{bmatrix} \ddot{\mathbf{q}}_u \\ \dddot{\mathbf{q}}_a \end{bmatrix} = \begin{bmatrix} \mathbf{M}_{uu}^{-1}\left(\mathbf{K}_u(\mathbf{q}) + \mathbf{G}_u(\mathbf{q}, \dot{\mathbf{q}})\right) - \mathbf{M}_{uu}^{-1}\mathbf{A}_{au}^T\ddot{\mathbf{q}}_a \\ -\frac{\ddot{\mathbf{q}}_a}{\tau} \end{bmatrix} + \begin{bmatrix} 0 \\ \frac{1}{\tau} \end{bmatrix} \ddot{\mathbf{q}}_a^{ref} \tag{7}$$

This model formulation fits the classical form of a set of first order ordinary differential equations usually adopted in control theory, with $\mathbf{u}$ the control vector and $\mathbf{x}$ the state vector:

$$\mathbf{u} = \ddot{\mathbf{q}}_a^{ref} \qquad \mathbf{x} = \begin{bmatrix} \dot{\mathbf{q}}_u \\ \ddot{\mathbf{q}}_a \end{bmatrix} \qquad \dot{\mathbf{x}} = \mathbf{f}(\mathbf{x}, t, \mathbf{u}) \tag{8}$$

2.1. Trajectory planning: variational formulation

This section proposes a solution to the problem of defining optimal trajectories for systems modeled as in Eq. (5) in point-to-point motion tasks. The problem is then extended to include robustness conditions as well. The method is proposed for point-to-point motions, i.e. when just the initial and final boundary conditions are imposed at the beginning and the end of the task. Between them, the planned trajectory is free and is chosen among the infinite trajectories connecting the two boundary points as the one minimizing a suitable scalar cost function J:

$$J = \int_{t_0}^{t_f} g(\mathbf{x}, t, \mathbf{u}) dt \tag{9}$$

A general formulation of J is proposed in Eq. (9) by means of an arbitrary function $g(\mathbf{x}, y, \mathbf{u})$ that is used to shape the properties of the resulting trajectory. Trajectory planning is therefore stated as the following constrained optimization problem:

$$\begin{cases} \min J(\mathbf{x}(t), t, \mathbf{u}) = \min \int_{t_0}^{t_f} g(\mathbf{x}, t, \mathbf{u}) dt \\ \\ \textit{subject to}: \\ \mathbf{x}(t_0) = \mathbf{x}_0 \\ \mathbf{x}(t_f) = \mathbf{x}_f \\ \dot{\mathbf{x}}(t) = \mathbf{f}(\mathbf{x}, t, \mathbf{u}) \end{cases} \tag{10}$$

The solution to the optimization problem of Eq. (10) leads to the definition of a trajectory $\mathbf{x}(t)$ that optimally drives the underactuated system from the configuration $\mathbf{x}_0$ at t_0 to the configuration $\mathbf{x}_f$ at time t_f while minimizing J. The solution to this problem can be found using the calculus of variations and Pontryagin's Minimum Principle (PMP) [43]. According to the common nomenclature, this kind of approach is commonly referred as the variational formulation to the trajectory planning [23]. This technique is of wide and convenient application for solving problems as in Eq. (10), since they can be solved numerically by either general purpose computing environments, such as MATLAB^{TM} [44] or optimization softwares such as PSOPT [45]. In the case of linear problems, the solution can also be found analytically in closed form [46] by using exponential matrices.

The optimization problem does not take into account the presence of any perturbations to the dynamic model expressed by Eq. (8). Hence the trajectory planning problem in Eq. (10) will be referred as the "nominal" problem, being based on the nominal model of Eq. (8). In order to tackle the presence of uncertainties, a "robust" problem can be defined by augmenting the formulation of Eq. (10) with the sensitivity functions computed with respect to some uncertain parameters.

The definition of the sensitivity functions and the proposed re-formulation of the problem are based on the method proposed in [32]. The developments are made with reference to a single uncertain parameter, since the extension to an arbitrary set of uncertain parameters is straightforward.

In the presence of uncertainty affecting an arbitrary parameter μ, the dynamic equation of the system can be written as:

$$\dot{\mathbf{x}}(t) = \mathbf{f}(\mathbf{x}, t, \mathbf{u}, \mu) \tag{11}$$

If $\mathbf{f}$ is continuous in $(\mathbf{x}, t, \mu)$ and is continuously differentiable with respect to $\mathbf{x}$ and μ for any value of $(\mathbf{x}, t, \mu)$ in the interval $[t_0, t]$, then the system response $\mathbf{x}(t, \mu)$ can be written as:

$$\mathbf{x}(t, \mu) = \mathbf{x}(t_0) + \int_{t_0}^{t} \mathbf{f}(s, \mathbf{x}(s), \mu) ds \tag{12}$$

The partial derivative of $\mathbf{x}(t, \mu)$, denoted $\mathbf{S}(t)$, made with respect to the uncertain parameter μ is used to describe the effects of the variation of the uncertain parameter on the system dynamics:

$$\mathbf{S}(t) = \frac{\partial \mathbf{x}(t)}{\partial \mu} = \int_{t_0}^{t} \left[\frac{\partial \mathbf{f}(s, \mathbf{x}(s,\mu), \mu)}{\partial \mathbf{x}} \mathbf{x}_\mu(s,\mu) + \frac{\partial \mathbf{f}(s, \mathbf{x}(s,\mu), \mu)}{\partial \mu} \right] ds \tag{13}$$

$\mathbf{S}(t)$ is the sensitivity function associated with the parameter μ, whose nominal value adopted in the nominal model is μ_0.

With the aim of incorporating enhanced robustness properties, the sensitivity function can be used to augment the optimization problem, which is now constrained by the augmented dynamics:

$$\dot{\mathbf{x}}^r(t) = \mathbf{f}^r(\mathbf{x}, \mathbf{S}, t, \mathbf{u}, \mu) = \left[\begin{array}{c} \mathbf{f}(\mathbf{x}, t, \mathbf{u}, \mu) \\ \dfrac{\partial \mathbf{f}(\mathbf{x}, t, \mathbf{u}, \mu)}{\partial \mu} \end{array} \right]_{\mu=\mu_0} ;$$

$$\mathbf{x}^r(t) := \left[\begin{array}{c} \mathbf{x}(t) \\ \mathbf{S}(t) \end{array} \right] \tag{14}$$

The complete reformulation of the nominal optimization problem of Eq. (10) is therefore:

$$\begin{cases} \min J^r(\mathbf{x}^r, t, \mathbf{u}) = \min \displaystyle\int_{t_0}^{t_f} g^r(\mathbf{x}^r, t, \mathbf{u}, \mu) dt \\ \textit{subject to}: \\ \mathbf{x}(t_0) = \mathbf{x}_0 \\ \mathbf{x}(t_f) = \mathbf{x}_f \\ \mathbf{S}(t_0) = 0 \\ \mathbf{S}(t_f) = 0 \\ \dot{\mathbf{x}}(t) = \mathbf{f}(\mathbf{x}(t), t, \mathbf{u}, \mu) \\ \dot{\mathbf{S}}(t) = \dfrac{\partial \mathbf{f}(\mathbf{x}(t), t, \mathbf{u})}{\partial \mu} \end{cases} \tag{15}$$

In other words, the robust optimization problem includes the additional constraints on the sensitivity function dynamics and the boundary values of the sensitivity functions, which are forced to be zero at the initial and final time. These additional boundary conditions are used to impose minimal sensitivity, i.e. maximum insensitivity, to the effects of the deviation of the nominal parameter μ from its nominal value μ_0.

As far as the solution of the augmented problem is concerned, standard methods employing the Pontryagin's Minimum Principle can be used [47, 23]. By defining the Hamiltonian of the system:

$$\mathcal{H} = g^r + \boldsymbol{\lambda}^T \mathbf{f}^r(\mathbf{x}^r, t, \mathbf{u}) \tag{16}$$

$\boldsymbol{\lambda} = [\lambda_1, \ldots, \lambda_N]^T$ is the vector of the Lagrangian multipliers, that has the same size as $\mathbf{x}^r$. The role of the Lagrangian multipliers is to specify that the optimization problem is constrained to the dynamics of system. The necessary conditions for the optimal solution of the problem of Eq. (15) are then:

$$\dot{\mathbf{x}} = \frac{\partial \mathcal{H}}{\partial \boldsymbol{\lambda}}; \quad \dot{\lambda} = -\frac{\partial \mathcal{H}}{\partial \mathbf{x}}; \quad \frac{\partial \mathcal{H}}{\partial \mathbf{u}} = 0; \tag{17}$$

Analytic solutions to this kind of problem are practically achievable only in a limited number of simple cases. For the other ones a numerical solution should be found by using collocation methods [48] or shooting methods [49].

3. Double pendulum crane: dynamic system

This section proposes the dynamic model of the system used for the experimental evaluation of the effectiveness of the proposed method. The system aims at replicating the dynamics of a double pendulum crane, which comprises of a cart which travels along the horizontal direction. The cart carries a double cascaded pendulum, built using two sections of fixed-length cable, whose lengths are L_1 and L_2. According to the nomenclature shown in Fig. 1, the position of the cart is denoted y_{cart}, while the two angular displacements of masses m_1 and m_2 are θ_1 and θ_2, respectively. The angle θ_1 is measured in an absolute reference frame, while the angle θ_2 is relative to θ_1. The horizontal position of the two masses are, in the same fashion, denoted y_1 and y_2, respectively. y_1 and y_2 are the two unactuated dofs, and the cart displacement y_{cart} is the only actuated one. The cart motion is imposed through the acceleration profile $\ddot{y}_{cart}(t)$.

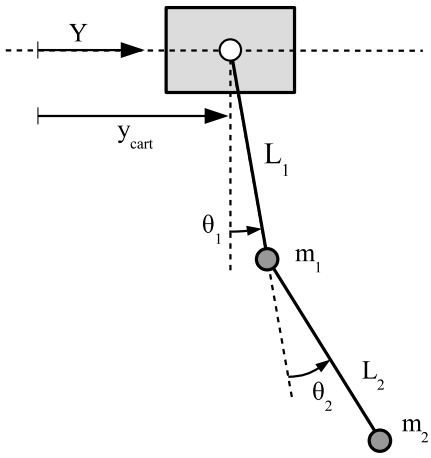

Figure 1: Kinematic model of the double pendulum crane used for the experiments

The dynamic model governing the motion of the unactuated subsystem, can be defined, using the Lagrangian formalism, as the set of the two second-order nonlinear differential equations:

$$\begin{aligned}&(m_1+m_2)\left[L_1\ddot{\theta}_1+gsin(\theta_1)\right]+\\&m_2L_2\left[\left(\ddot{\theta}_1+\ddot{\theta}_2\right)cos(\theta_2)-\left(\dot{\theta}_1+\dot{\theta}_2\right)^2sin(\theta_2)\right]\\&=\ddot{y}_{cart}\left(m_1+m_2\right)cos(\theta_1)\end{aligned} \tag{18}$$

$$\begin{aligned}&L_2\left(\ddot{\theta}_1+\ddot{\theta}_2\right)+g\sin(\theta_1+\theta_2)+\\&L_1\left[\dot{\theta}_1^2sin(\theta_2)+\ddot{\theta}_1cos(\theta_2)\right]\\&=\ddot{y}_{cart}cos(\theta_1+\theta_2)\end{aligned} \tag{19}$$

The state vector of the model in Eq. (7) is therefore assumed as:

$$\mathbf{x}(t)=\left[\ddot{y}_{cart},\dot{\theta}_1,\dot{\theta}_2\right]^T \tag{20}$$

and the exogenous input is $u(t)=\dddot{y}_{cart}(t)$. According to this re-definition of the input, the vector of actuated dofs will now include the cart acceleration, i.e. $\ddot{q}_a(t)=\ddot{y}_{cart}(t)$, while the vector of the underactuated dofs is $q_u(t)=[\theta_1(t),\theta_2(t)]^T$. According to the notation of Eq. (7), the dynamic model can be written using:

$$\mathbf{B}_a=1;\quad \mathbf{K}_a=0;\quad \mathbf{G}_a=0; \tag{21}$$

$$\mathbf{M}_{au} = \begin{bmatrix} L_1\left(m_1 + m_2\left(1 + L_2 cos(\theta_2)\right)\right) & m_2 L_2 cos(\theta_2) \\ L_1 cos(\theta_2) + L_2 & L_2 \end{bmatrix} \tag{22}$$

$$\mathbf{K}_u = \begin{bmatrix} -g(m_1+m_2)sin(\theta_1) + \ddot{y}_{cart}(m_1+m_2)cos(\theta_1) \\ -gsin(\theta_1+\theta_2) + \ddot{y}_{cart}cos(\theta_1+\theta_2) \end{bmatrix} \tag{23}$$

$$\mathbf{G}_u = \begin{bmatrix} m_2 L_2(\dot{\theta}_1^2 + \dot{\theta}_2^2)sin(\theta_2) \\ -L_1^2\dot{\theta}_1^2 sin(\theta_2) \end{bmatrix} \tag{24}$$

The first-order formulation of the model defined in Eq. (21-24) can be used to plan the trajectory according to equations (10) and (15). The latter is defined according to the definition of an uncertain parameter, which in this case is chosen as the length of the first cable L_1. The optimal trajectory will be therefore made robust against the deviation of L_1 from its nominal value, that might be due to an unmodeled change of such a length or an estimation error.

The dynamic model of the double pendulum crane should therefore be augmented with the sensitivity functions. It should be noted that the sensitivity functions corresponding to the motion of the cart, i.e. $\frac{\partial y_{cart}}{\partial L_1}$ and its time derivatives, can be omitted from the augmented model since they are always zero. Conversely, the dynamics of $\theta_1(t)$ and of $\theta_2(t)$ do depend on L_1. Therefore the state of the dynamic model used for the robust planning must be augmented as:

$$\mathbf{x}^r(t) = \left[\ddot{y}_{cart}, \dot{\theta}_1, \dot{\theta}_2, \dot{y}_{cart}, \theta_1, \theta_2, y_{cart}, \dot{s}_1, \dot{s}_2, s_1, s_2\right]^T \tag{25}$$

The additional sensitivity function are defined, according to Eq. (26) as:

$$\begin{aligned} s_1(t) &= \frac{\partial \theta_1(t)}{\partial L_1}; \qquad & s_2(t) &= \frac{\partial \theta_2(t)}{\partial L_1}; \\ \dot{s}_1(t) &= \frac{\partial \dot{\theta}_1(t)}{\partial L_1}; \qquad & \dot{s}_2(t) &= \frac{\partial \dot{\theta}_2(t)}{\partial L_1}; \end{aligned} \tag{26}$$

The functions $\dot{s}_1(t)$ and of $\dot{s}_2(t)$ are evaluated analytically according to Eq. (14).

4. Numerical results and comparison with input shaping

This section a compares the trajectories resulting form the application of the variational formulation proposed in the previous section and the ones resulting from three input shaping methods, which are assumed as the benchmark.

Input shaping consists in a re-definition of a reference profile by convolving it with a sequence of a finite number of impulses [13]. In other words, the trajectory actually fed to the mechanism is the linear combination of two or more repetitions shifted in time of the original one. This method can be applied to achieve some dynamic properties that the original trajectory cannot comply with. Usually the target is to achieve null residual vibrations. Such a condition can be achieved for any arbitrary original motion law, provided that the amplitude and the time delays of the convolved pulses are set correctly. Additionally, the plant must be described with sufficient accuracy by a the adopted linear model [14]. The most common solution is the the so-called Zero Vibration (ZV) shaper, which achieves null residual vibration by placing the second pulse half of the damped oscillation period after the first one [13]. Another option is to use a Negative Zero Vibration (NZV) shaper, which allows reducing the overall delay from half period to one third of the vibrational period [50]. These two methods are however quite affected by a limited robustness: a significant improvement can be achieved by using the solution provided by the Zero Vibration and Derivative (ZVD) shaper [50], which is also embodied in this work as a benchmark to establish a comparison with the robust variational formulation presented in the previous section. These three methods have been originally developed for a single mode oscillating system, but they all can be adapted to multi-mode systems simply by cascading several shapers, each individually tuned for the specific mode to be eliminated at the motion end, according to [13]. It should be

also noted that the three cited shaping methods are developed under the assumption of a linear behavior of the plant, and therefore they generally cannot ensure zero residual vibration when applied to control large oscillations of nonlinear systems, unlike the method proposed here.

A first comparison between the proposed method and some input shaping methods is reported in Fig. 2 and 3. The first one shows the speed and the acceleration profile obtained with the nominal vibration solution, as well as the one obtained with the ZV and NZV shaper. In the last two cases the shaping is obtained by filtering a fifth-order polynomial trajectory, chosen so that initial and final acceleration of the cart can be set to zero. The trajectories are designed to achieve a displacement of the cart equal to 0.3 m in 3 seconds. It should be pointed out that the ZV shaper introduces an overall delay equal to 1.211 s, i.e. the sum of the two half periods of the two modes of the system, according to the properties of the mechanism provided in Table 1. ω_1 and ω_2 are the oscillation frequencies of the double pendulum, evaluated by linearizing the model about the vertical equilibrium position ($\theta_1 = \theta_2 = 0$). In order to retain a total motion time equal to 3 s, the original unshaped fifth-order trajectory is designed to last 1.789 s. The negative input shaper is designed to introduce a delay equal to 0.808 s, and therefore the original unshaped trajectory is scaled to a total execution time equal to 2.192 s.

Parameter	Value	Unit
L_1	0.470	m
L_2	0.391	m
m_1	0.192	kg
m_2	0.201	kg
ω_1	3.640	rad/s
ω_2	9.017	rad/s

Table 1: Double-pendulum crane: model parameters

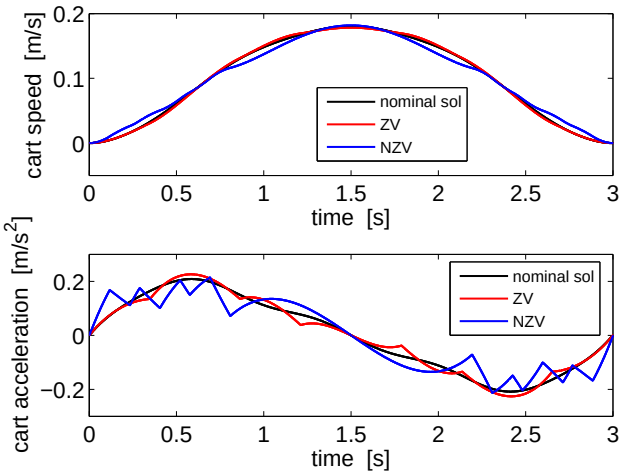

Figure 2: Speed and acceleration profiles: nominal variational solution, ZV and NZV shaper

Figure 2 shows that the three "nominal" trajectories lead to similar peak speed and accelerations. The application of the input shaping methods has also the drawback of losing the jerk continuity of the original fifth-order trajectory, thus leading to a motion profile that requires an high bandwidth servo-system for accurate tracking of the prescribed motion profile. Moreover, the execution time of the trajectory is lower bounded by the prescribed delay between the two convolving pulses when using the shaping, and therefore the absolute minimum execution times are 1.789 s and 0.808 s for the ZV and ZVD shaper, respectively. On the other hand, the solution

based on the variational formulation is not affected by this bound on the minimum completion time.

The solution to the variational formulation approach is obtained by imposing that the initial and final position of the cart are $y_{cart}(t_0) = 0$ and $y_{cart}(t_f) = 0.3$ m, respectively. The other elements of the state vector, as defined in Eq. (20) are set to zero both at initial and final time, in order to achieve initial and final acceleration of the cart as well as null residual vibrations starting from static conditions. The cost functional used in the solution of the nominal problem of Eq. (10) and of the robust problem of Eq. (15) is set as $g = 1/2\, \dddot{y}^2_{cart}$, therefore a minimum jerk problem is set-up and solved. Other countless choices are available: in particular it might be convenient to include in the cost function also the cart acceleration, which can be useful to cope with the bandwidth limitation of the servo system that drives the cart or to reduce the actuator effort.

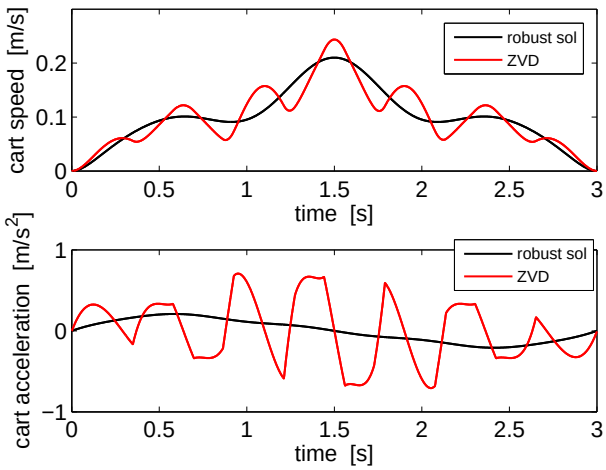

Figure 3: Speed and acceleration profiles: robust variational formulation and ZVD shaper

A similar comparison is set between the two robust solutions, namely the ZVD shaper and the robust variational formulation. The comparison in terms of cart speed and acceleration is provided in Fig. 3, for a trajectory that performs a cart translation equal to 0.3 m in 3 seconds, as in the previous case. The minimum motion time that can be be theoretically achieved with the ZVD shaper is equal to 2.432 s, i.e. the sum of the periods of oscillation of the two masses, as measured for small displacements. This constraint results in the highest values of speed and acceleration for any of the trajectories analyzed here. A more detailed comparison can be established using the data available in Tables 2 and 3, which list the main kinematic properties of the trajectories based on the nominal variational formulation and of the the robust variational approach, which are referred to as NVF and RVF, respectively. The properties of the trajectory designed using the three aforementioned shaping techniques are reported as well, and the are indicated by their common abbreviation, i.e. ZV, NZV and ZVD. Table 2 shows that the application of the ZVD shaper results in a peak acceleration that is roughly equal to 0.7 rad/s^2, while the robust variational formulation requires less than the half of that. The nominal variational solutions, as well as the ZV and NZV shaper require less than a third of the cart peak acceleration prescribed by the ZVD shaper. The estimated values of RMS acceleration show that, again, the application of the ZVD shaper is significantly less convenient than the application of the other methods. A less pronounced difference between the 5 trajectories is found between the peak and RMS values of the cart speed, again according to Tables 2 and 3.

4.1. Robustness analysis

A further comparison can be set among the considered trajectories to estimate the effects of an unmodeled perturbation to the system. Robustness has been estimated by the system response

to the planned trajectories with a varying cable length L_1, that is perturbed in the $\pm 30\%$ range from its nominal value, shown in Table 1.

Performances are assessed through the residual load swing, measured as the peak value of the oscillation of mass m_2 after motion completion. As expected, all the five methods lead to negligible residual load swing in the case of the nominal conditions $L_1 = 0.470$ m, and an increasing and slightly asymmetric performance degradation is encountered when the length of the first cable is either made longer or shorter. The results shown in Fig. 4 make evident that the nominal variational approach present a robustness property which is similar to the ones of the ZV and NZV trajectories, with a slight improvement over the ZV technique. A higher robustness is ensured for the robust variational formulation and for the ZVD solution, with the latter being less sensitive to variations of L_1. The sensitivity achieved by the variational formulation can also be modified by altering the optimization problem of Eq. (15): for example it has been observed that including the values of the sensitivities s_1 and s_2 in g' results in a lower overall sensitivity, at the cost of achieving higher peak values of cart acceleration and jerk. This feature is interesting since it gives more degrees of freedom in the design, to optimize the dynamic behavior or to choose the best trade-off between some conflicting performance specifications.

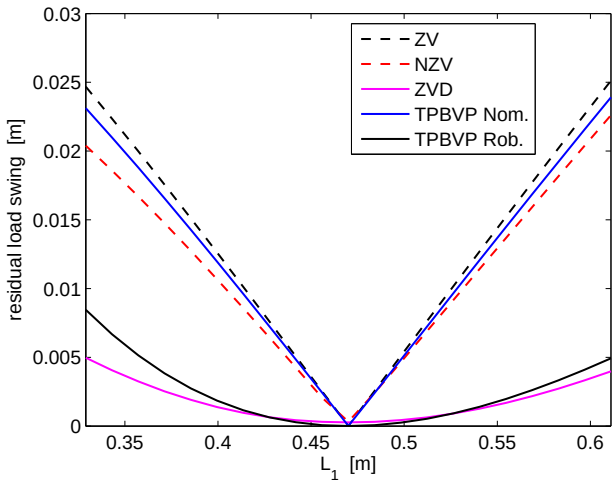

Figure 4: Comparison of peak residual load swing for $\pm 30\%$ variation on cable length L_1: variational approach versus input shaping

	$\dot{y}_{max}$	$\ddot{y}_{max}$	θ_{1max}	θ_{2max}
NVF	0.180517	0.208494	0.033474	8.5518e-03
RVF	0.210102	0.333652	0.026881	0.020872
ZV	0.178374	0.225946	0.034011	9.3271e-03
NZV	0.181720	0.214119	0.029477	6.2099e-03
ZVD	0.243682	0.706665	0.030016	0.027062

Table 2: Comparison between variational approaches and input shaping, for $T = 3$ s: peak values of kinematic variables

	$\dot{y}_{RMS}$	$\ddot{y}_{RMS}$	θ_{1RMS}	θ_{2RMS}
NVF	0.118199	0.135000	0.020983	4.7747e-03
RVF	0.113097	0.183944	0.015653	0.012426
ZV	0.129241	0.138253	0.023210	5.2253e-03
NZV	0.125924	0.128909	0.020116	3.8121e-03
ZVD	0.122832	0.395524	0.016201	0.012206

Table 3: Comparison between variational approaches and input shaping, for $T = 3$ s: RMS values of kinematic variables

5. Experimental results

The experimental validation of the effectiveness of the proposed method is proposed in this section together with the comparison with the input shaping methods. The double pendulum crane system is implemented by mounting a double pendulum with concentrated masses on the end-effector of an Adept Quattro s650h robot. Such a manipulator provides three translations and one rotation of the end effector, with high peak acceleration and speed. A picture of the manipulator used for the tests, together with the double pendulum, is shown in Fig. 5. The robot is controlled by the proprietary Adept SmartController. The robot controller is set-up so that the end-effector of the robot follows the trajectory profile supplied in real-time by an external trajectory generator implemented using MATLAB xPC Target, whose sample frequency is 1 kHz. Such a real-time device also takes care of collecting the measurements, which include the actual position of the end-effector of the robot and the angular displacement of the cable which connects mass m_1 with mass m_2, therefore providing a measurement of $\theta_1(t) + \theta_2(t)$. The measurement of the cable swing is performed using an artificial vision system, which analyzes the data acquired by a camera. The sampling frequency of the measured angular displacement is 50 Hz.

The communication between the xPC Target device and the robot controller is performed using the Ethernet protocol. This method, which is necessary to comply with the features of the robot controller, does not provide a deterministic timing and introduce a sensible delay. Therefore, the reference trajectory fed to the controller is a slightly distorted version of the one generated by the xPC Target device. Additionally, the interpolations made by the controller further introduce some modifications of the actual reference. This make the achievement of perfectly null residual vibration impossible in practice, especially when fast motions are performed.

Figure 5: Prototype of the double pendulum crane

5.1. Nominal plant

A first experimental comparison is set using the "nominal" plant in the trajectory generation, i.e. by setting the length of the two ropes and the weight of the masses as those in Table 1. All the trajectories are performed for $T = t_f - t_0 = 2.5$ s, which should be considered a high-speed motion in comparison with the load oscillation period. Indeed, faster trajectory can be handled by all the methods compared here, with the exception of the one generated by the ZVD shaper. The prescribed cart displacement is set to 0.3 m: the amplitude of this displacement is limited by the specifications of the camera used to measure the cable oscillation.

The first result is presented in Fig. 6, which shows the results of the application of the trajectory generated trough the solution of the nominal variational problem. This plot, as well as the following ones, shows the measured cart position y_{cart} fed back by the robot controller and the estimated horizontal positions of the two masses, which are indicated as y_1 and y_2, respectively. The latter measurements are performed by using an off-line estimation algorithm that implements an observer. The tuning of the observer is not critical, given the relative limited bandwidth of the oscillatory dynamics exhibited by the system.

Figure 6 presents also a magnified view of the masses oscillations in the ± 10 mm range, which show a residual oscillation that is roughly equal to ± 2 mm. This small residual vibration is mainly due to the unmodeled effects of the limited accuracy of the robot tracking system, as well as the effects of the trajectory distortion caused by the non-deterministic communication between the trajectory generator and the robot controller. However, the results are still very satisfactory given that the overall motion time is quite fast, being only marginally larger than the sum of the two period of oscillation of the double pendulum.

The signals shown in Fig. 7 have been obtained through the solution of the robust variational problem formulation. The resulting accuracy in achieving limited residual vibrations is higher than the one obtained in the previous case: the measured oscillation of the second mass is within the ± 1 mm range. This results indicates that, despite the higher peak acceleration required by the robust trajectory and the slightly lesser tracking precision, the prescribed final condition is obtained with more precision than in the previous case. Although not shown in the plots, the robust trajectory

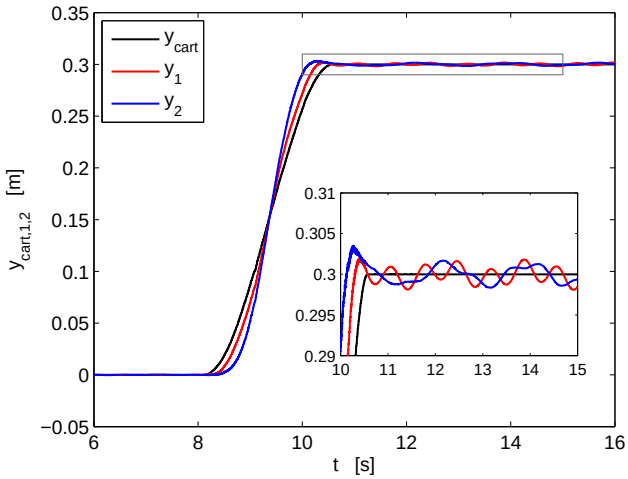

Figure 6: Experimental application of the nominal trajectory, variational approach for $T = 2.5$ s

requires higher peak acceleration of the cart, and therefore the robot robot position tracking is less precise than in the previous case.

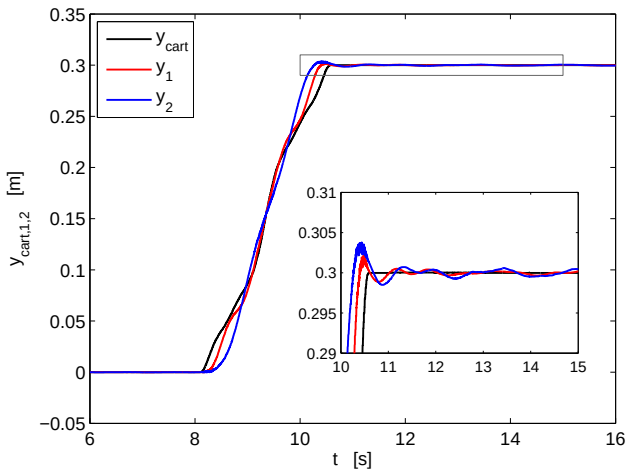

Figure 7: Experimental application of the robust trajectory, variational approach for $T = 2.5$ s

Good performances is achieved also when the trajectory generated by the ZV shaper is tested, as shown in Fig. 8: the peak amplitude of the residual vibrations is in this case slightly larger than the one obtained with the robust solution and slightly smaller than the one obtained with the solution to the nominal variational problem formulation.

A lesser accuracy is obtained for the trajectory produced by the NZV shaper, which has a peak of the residual vibration similar to the one obtained using by the nominal variational approach.

The negative shaper and the robust shaper produce trajectories that are more demanding in terms of trajectory tracking, when compared with the results presented above. In particular, the robust ZVD shaper, which is here operated close to its lower time bound, produces a pronounced residual oscillation, whose peak amplitude is close to 8 mm. The large amplitude of the load oscillations are also due to the limited accuracy of the linear approximation of the dynamic model that is needed to tune the shaper.

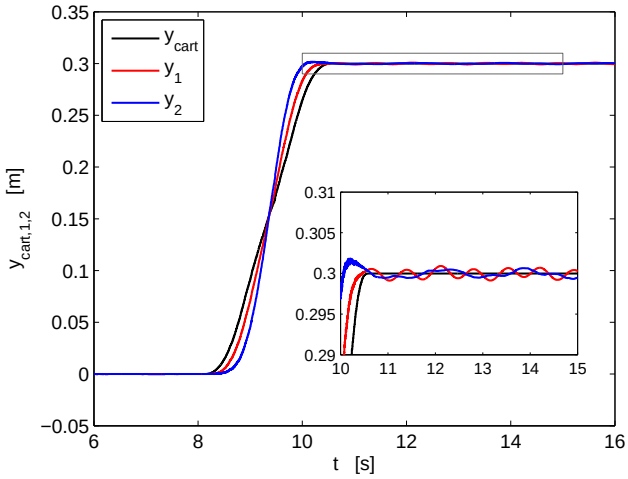

Figure 8: Experimental application of the trajectory obtained with the ZV shaper, for $T = 2.5$ s

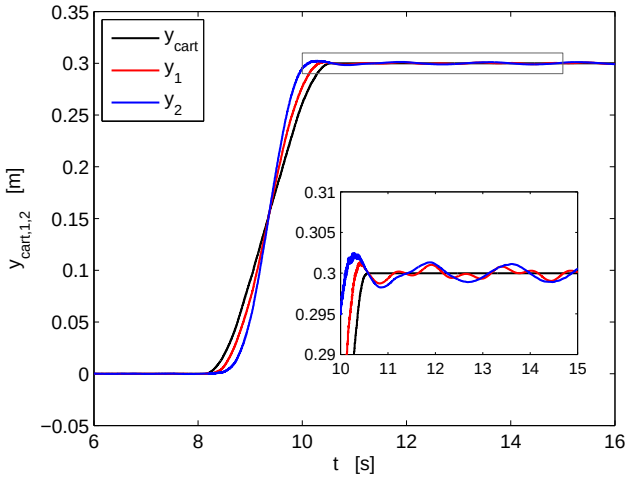

Figure 9: Experimental application of the trajectory obtained with the NZV shaper, for $T = 2.5$ s

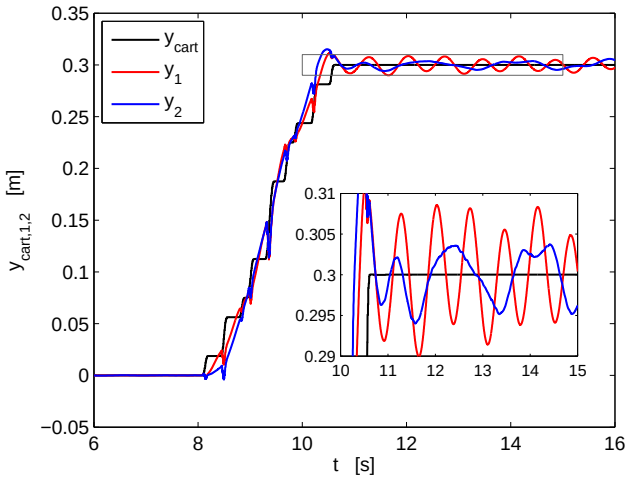

Figure 10: Experimental application of the trajectory obtained with the ZVD shaper, for $T = 2.5$ s

5.2. Perturbed system

The same trajectories already shown in figures 6-10 have been tested in the case of a perturbed plant. The length of the upper cable is shortened to 0.42 m, therefore causing a 3.11% increase to ω_1 and a 2.53% increase to ω_2. Despite the relatively small changes to the modal properties of the system, the amplitude of the residual vibration is sensibly larger for the nominal variational approach, as can be seen in Fig. 11. In contrast, the robust variational approach reacts effectively to the unmodeled change just by producing a slightly more pronounced residual oscillation compared with the unperturbed system, as from the direct comparison between the plots in Fig. 7 and 12.

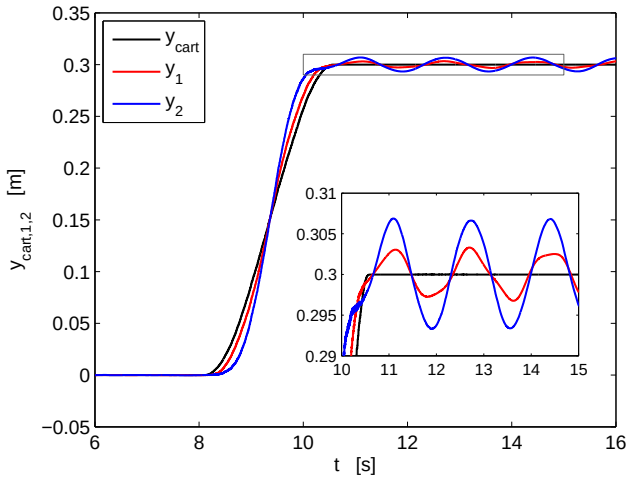

Figure 11: Experimental application of the nominal trajectory, variational approach for $T = 2.5$ s to the perturbed system

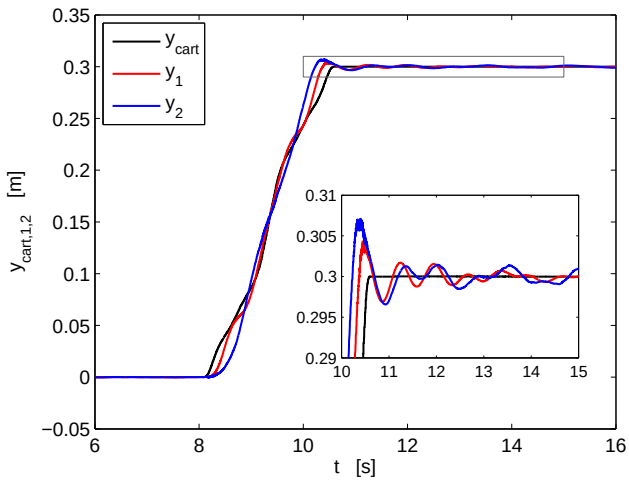

Figure 12: Experimental application of the robust trajectory, variational approach for $T = 2.5$ s to the perturbed system

The response to the nominal trajectory, obtained with the variational approach, as visible in Fig.11, can be compared with the equivalent experiment done with the ZV shaper, as in Fig. 13 and the NZV shaper, as in Fig. 14, as well. As predicted by the theoretical sensitivity shown in Fig. 4, the NZV shaper shows the most limited residual vibration amplitude among the three

non-robust methods. The largest residual oscillation are encountered when using the ZV shaper, while the nominal variational approach shows a slightly better performance than the ZV shaper, but still represents a sensible step-back in terms of robustness when compared with the robust variational approach.

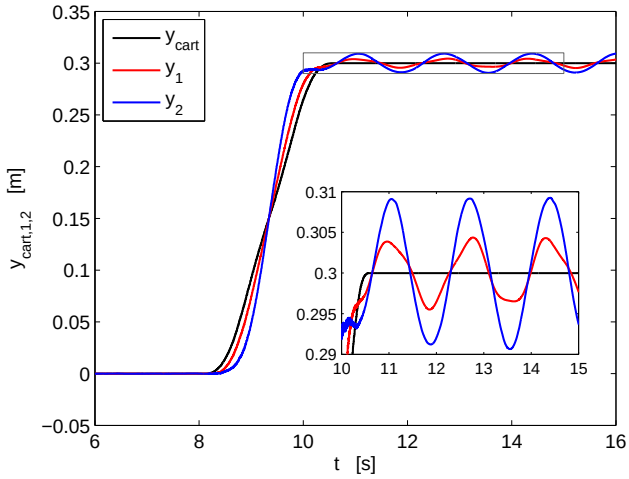

Figure 13: Experimental application of the trajectory obtained with the ZV shaper, for $T = 2.5$ s, to the perturbed system

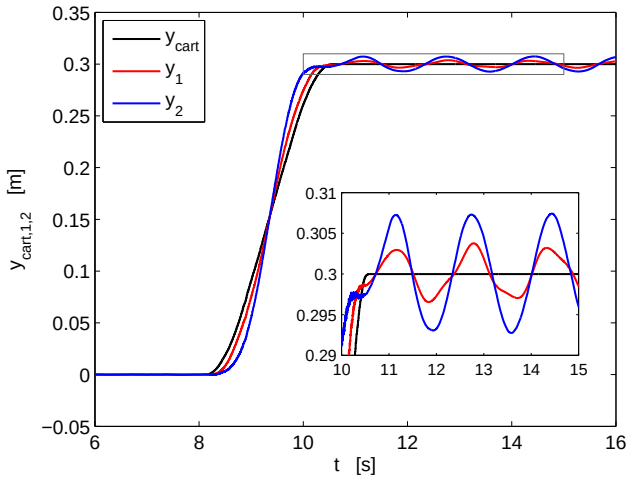

Figure 14: Experimental application of the trajectory obtained with the NZV shaper, for $T = 2.5$ s, to the perturbed system

As expected, and as shown by the results shown in Fig. 15, the unsatisfactory results shown by the application of the trajectory generated using the ZVD shaper to the nominal plant, are equally limited when applied to the perturbed plant. The comparison between the results in Fig. 12 and the ones in Fig. 10, makes evident that the proposed robust variational approach to the definition of trajectories is of convenient application when the motion task is to be completed within a time durations that is similar to, or even smaller than the oscillation period. Moreover, the gap between the performances of the proposed variational approach and the input shaping methods is reasonably expected to be wider in the cases in which the nonlinear effects of the dynamics, that are neglected in the classical input shaping framework, are more relevant.

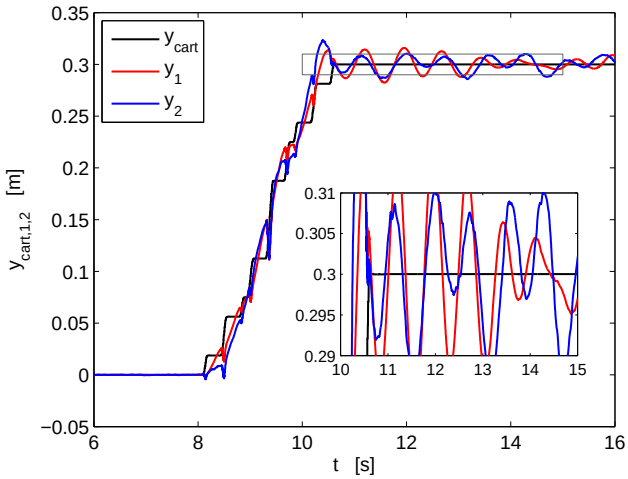

Figure 15: Experimental application of the trajectory obtained with the NZV shaper, for $T = 2.5$ s, to the perturbed system

Further results are presented in Fig. 16, which shows the measured peak values of the load swing when altering the length of the cable L_1 in the $\pm$ 30% range from its nominal value. Each point of the graph is obtained by averaging the outcome of six repetitions of the same test. The results provide experimental evidence of the reduced sensitivity to model uncertainties when the robust shaper and the robust variational solutions are tested, given that a significant alteration to the oscillating mode of the system corresponds, in both cases, to an increase of the residual oscillation that is a most equal to 7 mm. Such measure is in good agreement with the numerical results presented in Fig. 4. Figure 16 shows that the effectiveness of the ZVD shaper is however severely affected by the limited bandwidth of the robot position tracking system, since the best achievable residual load swing is never smaller than 8 mm. Such a limitation is less relevant when the other techniques are used, since the experimental results are in good agreement with the nominal ones presented in section 4.1 and in Fig. 4.

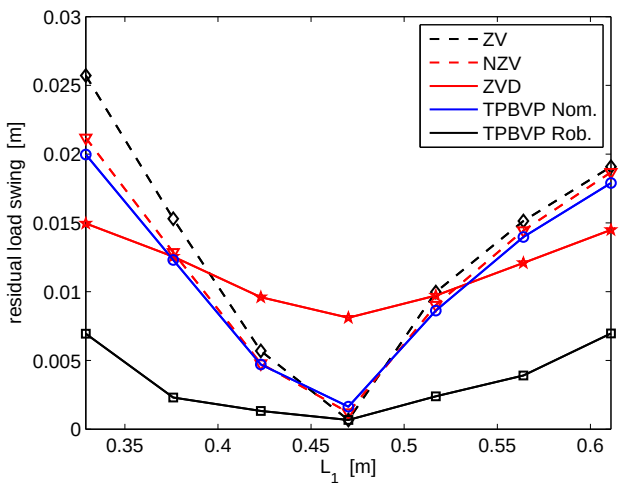

Figure 16: Comparison of peak residual load swing for $\pm$ 30% variation on cable length L_1: experimental results

6. Conclusion

This paper proposed the experimental validation of a model-based robust trajectory planning method for nonlinear systems. Compared with a standard variational formulation, the tested method allows improving the parametric robustness through the inclusion of additional constraints on the sensitivity functions of the model used for trajectory planning. The improved robustness is proved through the analysis of the residual vibration in a rest-to-rest motion for a double pendulum crane, showing that the method allows for the reduction the effect of unmeasured changes to the properties of the plant. A comparison is also set with three well-established input shaping methods, showing that the proposed solution offers better performances, especially when fast motion is required. In particular, the robust variational formulation leads to a trajectory that is easier to track than the equivalent one obtained with the robust ZVD shaper for motion times that are close to the sum of the two periods of oscillation of the system. This feature has positive effects on the overall motion accuracy and on the residual vibrations.

[1] M. Benosman, G. Le Vey, Control of flexible manipulators: A survey, Robotica 22 (05) (2004) 533–545.

[2] L. Biagiotti, C. Melchiorri, Trajectory planning for automatic machines and robots, Springer Science & Business Media, 2008.

[3] A. Abe, An effective trajectory planning method for simultaneously suppressing residual vibration and energy consumption of flexible structures, Case Studies in Mechanical Systems and Signal Processing 4 (2016) 19–27.

[4] A. Ata, Optimal trajectory planning of manipulators: a review, Journal of Engineering Science and Technology 2 (1) (2007) 32–54.

[5] B. Siciliano, O. Khatib, Springer handbook of robotics, Springer-Verlag New York Inc, 2008.

[6] R. Bearee, A. Olabi, Dissociated jerk-limited trajectory applied to time-varying vibration reduction, Robotics and Computer-Integrated Manufacturing 29 (2) (2013) 444–453.

[7] A. Gasparetto, V. Zanotto, A new method for smooth trajectory planning of robot manipulators, Mechanism and Machine Theory 42 (4) (2007) 455–471.

[8] A. Gasparetto, A. Lanzutti, R. Vidoni, V. Zanotto, Experimental validation and comparative analysis of optimal time-jerk algorithms for trajectory planning, Robotics and Computer-Integrated Manufacturing 28 (2) (2012) 164–181.

[9] W. Aribowo, K. Terashima, Cubic spline trajectory planning and vibration suppression of semiconductor wafer transfer robot arm, International Journal of Automation Technology 8 (2) (2014) 265–274.

[10] N. Uchiyama, S. Shigenori, K. Haneda, Residual vibration suppression using simple motion trajectory for mechanical systems, SICE Journal of Control, Measurement, and System Integration 8 (3) (2015) 195–200.

[11] R. Bearee, New damped-jerk trajectory for vibration reduction, Control Engineering Practice 28 (2014) 112–120.

[12] C. T. Kiang, A. Spowage, C. K. Yoong, Review of control and sensor system of flexible manipulator, Journal of Intelligent & Robotic Systems 77 (1) (2015) 187–213.

[13] W. Singhose, Command shaping for flexible systems: A review of the first 50 years, International Journal of Precision Engineering and Manufacturing 10 (4) (2009) 153–168.

[14] N. C. Singer, W. P. Seering, et al., Preshaping command inputs to reduce system vibration, Massachusetts Institute of Technology, Artificial Intelligence Laboratory, 1988.

[15] T. D. Tuttle, W. P. Seering, A zero-placement technique for designing shaped inputs to suppress multiple-mode vibration, in: American Control Conference, 1994, Vol. 3, IEEE, 1994, pp. 2533–2537.

[16] L. Y. Pao, T. N. Chang, E. Hou, Input shaper designs for minimizing the expected level of residual vibration in flexible structures, in: American Control Conference, 1997. Proceedings of the 1997, Vol. 6, IEEE, 1997, pp. 3542–3546.

[17] L. Biagiotti, C. Melchiorri, FIR filters for online trajectory planning with time-and frequency-domain specifications, Control Engineering Practice 20 (12) (2012) 1385–1399.

[18] P. Besset, R. Bearée, O. Gibaru, FIR filter-based online jerk-controlled trajectory generation, in: Industrial Technology (ICIT), 2016 IEEE International Conference on, IEEE, 2016, pp. 84–89.

[19] D. Hull, Conversion of optimal control problems into parameter optimization problems, Journal of guidance, control, and dynamics 20 (1) (1997) 57–62.

[20] A. Abe, K. Hashimoto, A novel feedforward control technique for a flexible dual manipulator, Robotics and Computer-Integrated Manufacturing 35 (2015) 169–177.

[21] H. Kojima, T. Kibe, Optimal trajectory planning of a two-link flexible robot arm based on genetic algorithm for residual vibration reduction, in: IEEE/RSJ International Conference on Intelligent Robots and Systems, Vol. 4, 2001, pp. 2276–2281.

[22] M. Korayem, A. Nikoobin, V. Azimirad, Trajectory optimization of flexible link manipulators in point-to-point motion, Robotica 27 (6) (2009) 825–840.

[23] D. Kirk, Optimal control theory: an introduction, Dover Publications, 2004.

[24] D. Balkcom, M. Mason, Time optimal trajectories for bounded velocity differential drive vehicles, The International Journal of Robotics Research 21 (3) (2002) 199–217.

[25] O. Dahl, Path constrained motion optimization for rigid and flexible joint robots, in: International Conference on Robotics and Automation, Vol. 2, IEEE, 1993, pp. 223–229.

[26] P. Boscariol, A. Gasparetto, Model-based trajectory planning for flexible-link mechanisms with bounded jerk, Robotics and Computer-Integrated Manufacturing 29 (4) (2013) 90–99.

[27] M. Bamdad, Time-energy optimal trajectory planning of cable-suspended manipulators, in: Cable-Driven Parallel Robots, Springer, 2013, pp. 41–51.

[28] D. J. McKeown, W. J. O'Connor, Wave-based control-implementation and comparisons, in: American Control Conference, 2007. ACC'07, IEEE, 2007, pp. 4209–4214.

[29] D. Gallardo, O. Colomina, F. Flórez, R. Rizo, A genetic algorithm for robust motion planning, in: International Conference on Industrial, Engineering and Other Applications of Applied Intelligent Systems, Springer, 1998, pp. 115–121.

[30] K. Shin, N. McKay, Robust trajectory planning for robotic manipulators under payload uncertainties, IEEE transactions on Automatic Control 32 (12) (1987) 1044–1054.

[31] B. Houska, Robust optimization of dynamic systems, Ph.D. thesis, PhD thesis, Katholieke Universiteit Leuven, 2011.(ISBN: 978-94-6018-394-2) (2011).

[32] P. Boscariol, A. Gasparetto, Robust model-based trajectory planning for nonlinear systems, Journal of Vibration and Control 22 (18) (2016) 3904–3915.

[33] T. Singh, Optimal reference shaping for dynamical systems: theory and applications, CRC Press, 2009.

[34] R. Kased, T. Singh, Rest-to-rest motion of an experimental flexible structure subject to friction: Linear programming approach, Journal of Vibration and Acoustics 132 (1) (2010) 011005.

[35] A. A. Ata, Inverse dynamic analysis and trajectory planning for flexible manipulator, Inverse Problems in Science and Engineering 18 (4) (2010) 549–566.

[36] A. De Luca, G. Di Giovanni, Rest-to-rest motion of a two-link robot with a flexible forearm, in: Advanced Intelligent Mechatronics, 2001. Proceedings. 2001 IEEE/ASME International Conference on, Vol. 2, IEEE, 2001, pp. 929–935.

[37] G. Bastos, R. Seifried, O. Brüls, Analysis of stable model inversion methods for constrained underactuated mechanical systems, Mechanism and Machine Theory 111 (2017) 99–117.

[38] Z. Wu, X. Xia, Optimal motion planning for overhead cranes, IET Control Theory & Applications 8 (17) (2014) 1833–1842.

[39] N. Sun, Y. Fang, Y. Zhang, B. Ma, A novel kinematic coupling-based trajectory planning method for overhead cranes, IEEE/ASME Transactions on Mechatronics 17 (1) (2012) 166–173.

[40] H.-H. Lee, Motion planning for three-dimensional overhead cranes with high-speed load hoisting, International Journal of Control 78 (12) (2005) 875–886.

[41] R. Zanasi, C. G. L. Bianco, A. Tonielli, Nonlinear filters for the generation of smooth trajectories, Automatica 36 (3) (2000) 439–448.

[42] P. Barre, R. Bearee, P. Borne, E. Dumetz, Influence of a jerk controlled movement law on the vibratory behaviour of high-dynamics systems, Journal of Intelligent & Robotic Systems 42 (3) (2005) 275–293.

[43] D. S. Naidu, Optimal control systems, CRC press, 2002.

[44] D. Garg, M. A. Patterson, C. Francolin, C. L. Darby, G. T. Huntington, W. W. Hager, A. V. Rao, Direct trajectory optimization and costate estimation of finite-horizon and infinite-horizon optimal control problems using a radau pseudospectral method, Computational Optimization and Applications 49 (2) (2011) 335–358.

[45] V. M. Becerra, R. K. H. Galvão, A tutorial on pseudospectral methods for computational optimal control, Sba: Controle & Automação Sociedade Brasileira de Automatica 21 (3) (2010) 224–244.

[46] S. Agrawal, T. Veeraklaew, A higher-order method for dynamic optimization of a class of linear systems, Journal of dynamic systems, measurement, and control 118 (1996) 786–790.

[47] L. Pontryagin, R. Gamkrelidze, The mathematical theory of optimal processes, Vol. 4, CRC, 1986.

[48] L. Shampine, I. Gladwell, S. Thompson, Solving ODEs with MATLAB, Cambridge University Press, 2003.

[49] R. W. Holsapple, A modified simple shooting method for solving two-point boundary value problems, Ph.D. thesis, Texas Tech University (2003).

[50] W. Singhose, E. O. Biediger, Y.-H. Chen, B. Mills, Reference command shaping using specified-negative-amplitude input shapers for vibration reduction, Transactions-american society of mechanical engineers journal of dynamic systems measurement and control 126 (1) (2004) 210–214.